Journal of Marine Science and Technology

Volume 31 | Issue 4 Article 12

ARTIFICIAL INTELLIGENCE IN PREDICTION OF THE REMAINING USEFUL LIFE OF WIND TURBINE SHAFT BEARINGS

Jinsiang Shaw
Institute of Mechatronic Engineering, jshaw@ntut.edu.tw

B.J. Wu
Research Center of Energy Conservation for New Generation of Residential, Commercial, and Industrial Sectors

Recommended Citation

Shaw, Jinsiang and Wu, B.J. (2023) "ARTIFICIAL INTELLIGENCE IN PREDICTION OF THE REMAINING USEFUL LIFE OF WIND TURBINE SHAFT BEARINGS," *Journal of Marine Science and Technology*: Vol. 31: Iss. 4, Article 12.
DOI: 10.51400/2709-6998.2719
Available at: https://jmstt.ntou.edu.tw/journal/vol31/iss4/12

RESEARCH ARTICLE

Artificial Intelligence in Prediction of the Remaining Useful Life of Wind Turbine Shaft Bearings

Jinsiang Shaw [a,b,*], Bingjie Wu [a]

[a] Institute of Mechatronic Engineering, National Taipei University of Technology, Taipei, Taiwan
[b] Research Center of Energy Conservation for New Generation of Residential, Commercial, and Industrial Sectors, National Taipei University of Technology, Taipei, Taiwan

Abstract

Long-term periodic rotation and unstable load changes in wind turbines can cause unexpected damage to high-speed shaft bearings (HSSBs). In this study, after preprocessing of the HSSB vibration signal, four different models for predicting bearing degradation in terms of remaining useful life (RUL) in days were investigated: support vector regression (SVR), convolutional neural networks (CNN), long short-term memory (LSTM), and CNN-LSTM. The experimental results revealed that the CNN achieved the best mean absolute error (MAE), at 0.44 days, based on frequency response plot using the fast Fourier transform (FFT), while that of the CNN-LSTM model predicted using the amplitude profile in frequency response was 1.24 days. Meanwhile, the MAE of the SVR that extracted a total of 15 features for prediction was 2.31 days, while that of the LSTM predicted with the original time-domain data was 14.93 days, which was the worst. The experimental results demonstrated that, compared to the traditional time-domain vibration characteristics, the FFT-based method can predict the degradation trend of HSSBs more accurately.

Keywords: RUL, Deep learning, Regression prediction

1. Introduction

Wind turbines are major components of the current green energy market. Wind energy development occurs onshore, offshore, and in deep-sea areas [1]. Generally, the actual service life of a wind turbine gearbox is shorter than its design life of 20 years, and faults mainly lie in the positions of the planetary bearings, intermediate shafts, and high-speed shaft bearings (HSSBs). This is because the rotor bearings support the main shaft and blades, which apply loads in the dynamic axial and radial directions and operate at low speeds of 20−30 rpm. As such, periodic loads are applied to the bearings, which can bend the main shaft. In turn, this can lead to bearing misalignment, which may cause long-term damage, and the medium- and high-speed bearings in the gearbox may also deteriorate [2−4].

Vibration analysis is a monitoring technology commonly used in rotating machinery in the industry and is also an effective method for checking bearing failures. Various bearing detection approaches have been proposed by Yang et al. [5], Saidi and Fnaiech [6], and Ben Ali et al. [7].

Based on the method of spectral kurtosis (SK) presented by Saidi et al. [8], the one-dimensional feature vector related to the vibration signals served as the input to the support vector regression (SVR) for HSSB life prediction. The experimental results show that SK contributes to early warning. Subsequently, one-dimensional convolutional neural networks (CNNs) and recurrent neural networks (RNNs) [9,10] that are combined for life prediction. A CNN was used as an automatic feature extractor [11], while an RNN is employed to extract the prior and posterior features of the sequence. This combined method obtained a considerably high prediction

Received 1 May 2023; revised 5 November 2023; accepted 6 November 2023.
Available online 15 December 2023

* Corresponding author at: Research Center of Energy Conservation for New Generation of Residential, Commercial, and Industrial Sectors, National Taipei University of Technology, Taipei, Taiwan.
E-mail address: jshaw@ntut.edu.tw (J. Shaw).

https://doi.org/10.51400/2709-6998.2719

accuracy. In addition, by converting the one-dimensional vibration signal to a two-dimensional frequency response plot, the CNN was used to predict fault diagnosis and shown to have a significant effect on prediction accuracy [12]. A recent study by Merainani et al. [13] proposed a practical and effective data-driven methodology that can be applied to the RUL prediction of HSSBs. It first involves preprocessing using the Teager energy operator, followed by extraction of the relevant statistical features from the spectral shape factor (SSF), and finally used as an input to an Elman neural network for RUL estimation. The experimental results show that the proposed approach can provide effective RUL estimation with good accuracy.

This study mainly aimed to process the vibration signals of HSSBs in different domains and establish four predictive models, SVR, CNN, LSTM, and CNN-LSTM, to predict RUL. Finally, the MAE of each model was compared to evaluate its performance. It should be noted that this study is a sequel to the authors' previous work, in which a support vector machine (SVM) and CNN were applied to predict the RUL in classification rather than a regression problem [14]. The remainder of this paper is organized as follows: Section 2 introduces basic information regarding the SVR, CNN, and LSTM regression models used in this study. Section 3 describes different approaches for obtaining features as inputs for the investigated models. Moreover, a thorough comparison of the MAE results of the RUL obtained using each model is presented. Finally, Section 4 concludes the paper.

2. Regression model

2.1. Support vector regression (SVR)

SVR operates in the same manner as SVM; both project the original data into a high-dimensional feature space to find an optimal hyperplane for the accurate prediction of data labels.

Fig. 1 shows that, when extensive data exist on a feature plane, SVR attempts to determine the optimal margin whereby the data points can be accurately classified. The regression hyperplane is determined such that the farthest point from the datacenter is at the largest distance from it. Two dashed lines indicate that the black dot errors between them are zero. The distance between the dashed line and data outside it is the error "ξ." Predictive regression tries to minimize ξ. The dashed lines H1 and H2 are called support hyperplanes,

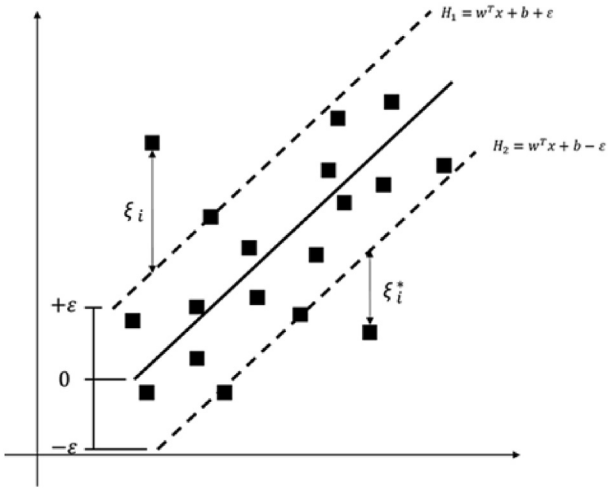

Fig. 1. Support vector regression (SVR) example diagram.

while ϵ indicates the maximum distance between the SVR predicted and actual values [15].

2.2. Convolutional neural network (CNN)

A CNN is a feed-forward neural network. In 1998, Yann LeCun proposed the original CNN architecture, called LeNet-5 [16]. In 2012, AlexNet, another CNN method, won the famous ImageNet large-scale visual recognition challenge (ILSVRC). Subsequently, various other types of CNN architectures have been developed, such as NfNet, VggNet, GoogleNet, and ResNet, which are widely used for image recognition tasks [22].

Fig. 2 shows the LeNet-5 architecture. The input image passes through the convolutional and sampling layers sequentially (subsampling layer), followed by two fully connected layers, and finally a Gaussian connection output. Among them, the convolution and subsampling layers extract the low-level features of the image, which play the most important role in CNNs and are different from those in typical neural networks.

2.3. Long short-term memory (LSTM)

The LSTM network, first introduced by Hochreiter and Schmidhuber [17], is a time-sequential network improved from an RNN by modifying the hidden layer. Three new gates are introduced: the input, output, and forget gates. The same prior hidden states H and C are captured, with the difference that H and C are short- and long-term memories, respectively. The LSTM structure is illustrated in Fig. 3.

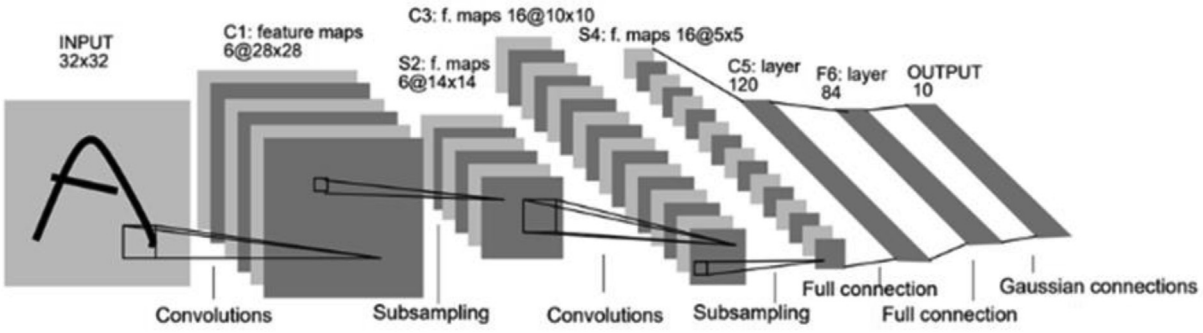

Fig. 2. LeNet-5 architecture.

3. Experimental results

3.1. Experimental data

The vibration data used in our experiment were collected on-site using a 2 MW commercial wind turbine. The US Green Power Monitoring System provided real-world WTG high-speed bearing data [18]. The bearing model was an SKF 32222 J2 tapered roller bearing.

3.2. Feature extraction

Each day, 585,936 vibration data samples from normal (Day 1) to damaged (Day 50) were collected over 6 s with a 97,656 Hz sampling frequency for a total of 50 days, as shown in Fig. 4. To determine the signs of HSSB degradation, statistical time-domain features, such as root mean square, standard deviation, skewness, and shape factor, can be used. In addition, SK is included as another reference indicator that can extract the impact signal covered by strong noise from the rotating machinery. SK is strongly capable of filtering out faulty mechanical features at an early stage [19] and is defined as follows:

$$\mathrm{SK}(f)=\frac{\langle|X^4(t,f)|\rangle}{\langle|X^4(t,f)|\rangle^2}-2 \tag{1}$$

where <.> is the time-frequency averaging operator [8]. Once the signal is extracted by SK, the skewness, kurtosis, mean, and standard deviation are estimated and included in the input feature vector for RUL prediction.

To perform frequency analysis, the vibration data for each day were converted to the frequency domain using a fast Fourier transform (FFT) to obtain a spectrogram. As shown in Fig. 5(a) and (b), comparison between the 25th and 50th days reveals that the main energy between 8000 and 12,000 Hz has an increasing trend as the testing days progress, which can serve as a basis for prediction.

3.3. Predicted regression model setup

In this study, we built four different models: SVR, CNN, LSTM, and CNN-LSTM. To compare the

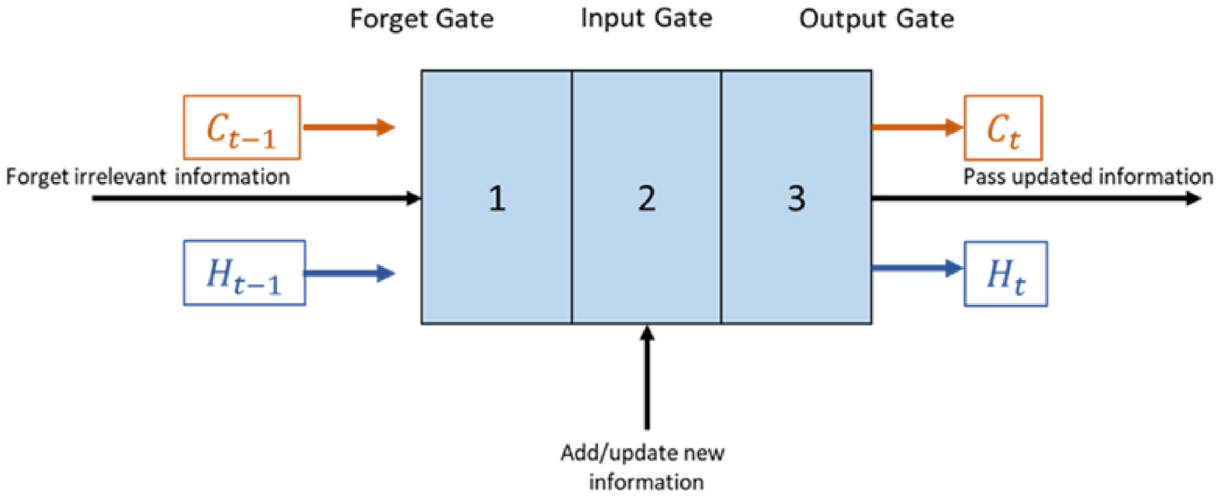

Fig. 3. Long short-term memory (LSTM) architecture.

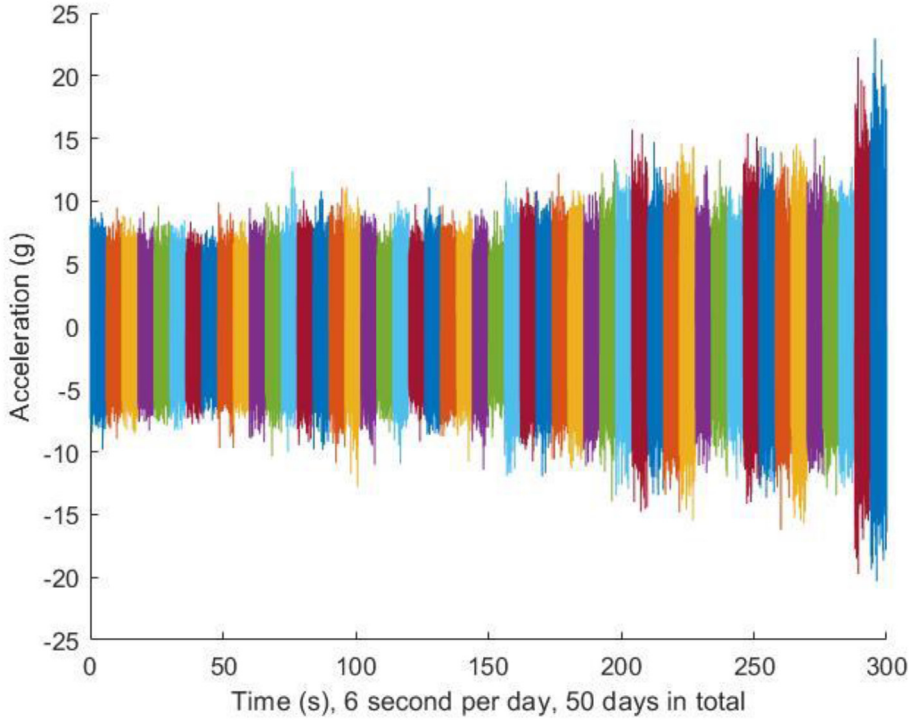

Fig. 4. Run-to-failure vibration signal in the time-domain.

performances among these models, MAE was adopted, defined as follows:

$$\mathrm{MAE} = \frac{\sum_{i=1}^{n} |e_i|}{n} \tag{2}$$

where e_i is the error between the predicted and true values, and n is the sample number. The neural model layer configurations are presented in Table 1. Specifically, the CNN-LSTM has been employed in several previous studies, while CNN plus LSTM demonstrated better prediction results regarding time-sequential data [10,20]; thus, it is included here for performance evaluation.

3.4. RUL predictions

The RUL is defined as RUL (days) = 50 − the days the data were sampled. The input data for the SVR

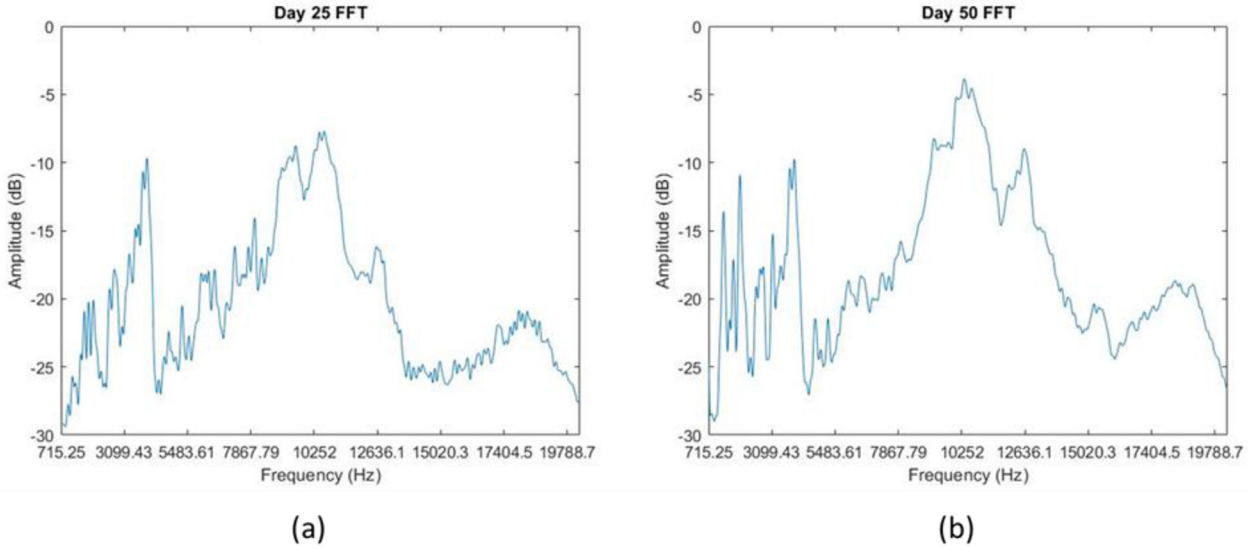

Fig. 5. Spectrograms for (a) Day 25 and (b) Day 50.

Table 1. Layer configuration of each model.

Layer name	CNN	LSTM	CNN-LSTM
L1	Conv2D (3 × 3 × 32)	LSTM(100)	Conv1D (8 × 64)
L2	BatchNormalization ()	Dropout (0.2)	MaxPooling1D (2)
L3	MaxPooling2D (2 × 2)	Dense (1)	Conv1D (1 × 3)
L4	Dropout (0.25)		MaxPooling1D (2)
L5	Conv2D (3 × 3 × 64)		Conv1D (1 × 3)
L6	BatchNormalization ()		MaxPooling1D (2)
L7	MaxPooling2D (2 × 2)		Conv1D (1 × 3)
L8	Dropout (0.25)		MaxPooling1D (2)
L9	Conv2D (3 × 3 × 128)		Conv1D (1 × 3)
L10	BatchNormalization ()		MaxPooling1D (2)
L11	MaxPooling2D (2 × 2)		Conv1D (1 × 3)
L12	Dropout (0.25)		MaxPooling1D (2)
L13	Dense (256)		LSTM(256)
L14	BatchNormalization ()		Dense (100)
L15	Dropout (0.5)		Dense (1)
L16	Dense (128)		
L17	BatchNormalization ()		
L18	Dropout (0.5)		
L19	Dense (1)		

is a vector with 15 features. Eleven time-domain features and four SK features were extracted from the original time-domain data, which have been proven to be effective in indicating complex bearing faults and are independent of the shaft speeds and loads [8,21]. Nine of the ten groups on each day were used for multi-SVR training. Once the training phase was completed, the remaining groups served as the test data for each day. We used three different kernel functions for SVR: linear, polynomial, and Gaussian. The final MAEs obtained for the RUL were 4.14, 2.70, and 2.31 days for the linear, polynomial, and Gaussian kernels, respectively. Fig. 6 shows the best RUL predictions of SVR with the Gaussian kernel function, where the red straight line represents the ground truth RUL, and the blue line indicates the RUL predicted by the model. Saidi et al. [8] applied an SVR model to predict the RUL of the same HSSB system. The data from the first 30 days (60 %) were used for training, while the last 20 days (40 %) were reserved for testing. The testing errors in the RUL predictions are similar to those shown in Fig. 6.

The CNN model uses spectrogram images as input. The captured frequency range was 715−24414 Hz, with 30 frames collected daily. A total of 1500 images were divided into training and testing groups with 1450 and 50 images, respectively. After 500 training epochs, the test MAE of RUL was 0.44 days, and the corresponding prediction results are given in Fig. 7.

For the LSTM model input, 1000 randomly extracted consecutive points from the original data were used. Each day, 50 groups were extracted, and a total of 2500 groups were used for training, with the input matrix dimension being (2500, 1000, 1). After 100 training iterations, the obtained MAE of the RUL was 14.93 days. Fig. 8 shows the predicted results.

The training and testing groups used in the CNN model were reused here for the CNN-LSTM model. However, the training samples passed to the CNN-LSTM model had a one-dimensional amplitude profile in the spectrogram, which were collected with a frequency range of 715−24414 Hz, taking 1989 points in total. The input training matrix had a shape of (1450, 1989, 1), and after training, the CNN-LSTM predicted the RUL with an MAE of 1.24 days. The corresponding prediction results are presented in Fig. 9. Table 2 lists the MAEs of predicted models.

3.5. Discussions

The best results for RUL prediction were obtained by the CNN, with a spectrogram as its input. The RUL prediction graph is mostly consistent with the true RUL. Compared with CNN-LSTM, it requires one step (FFT) to convert the data into a graph. Conversely, CNN-LSTM only requires 1-dimensional frequency domain data to obtain good results. However, the prediction misalignment in the last three days of the CNN-LSTM model must be considered. The possible mechanism behind the prediction misalignment as time approaches the end of HSSBs' life is explained as follows: the one-dimensional amplitude profile in the frequency domain becomes larger in amplitude range with more oscillations compared to its predecessors. This is illustrated in Fig. 5. Therefore, it is more difficult for the CNN-LSTM model to learn the features in the last three days of HSSBs' life.

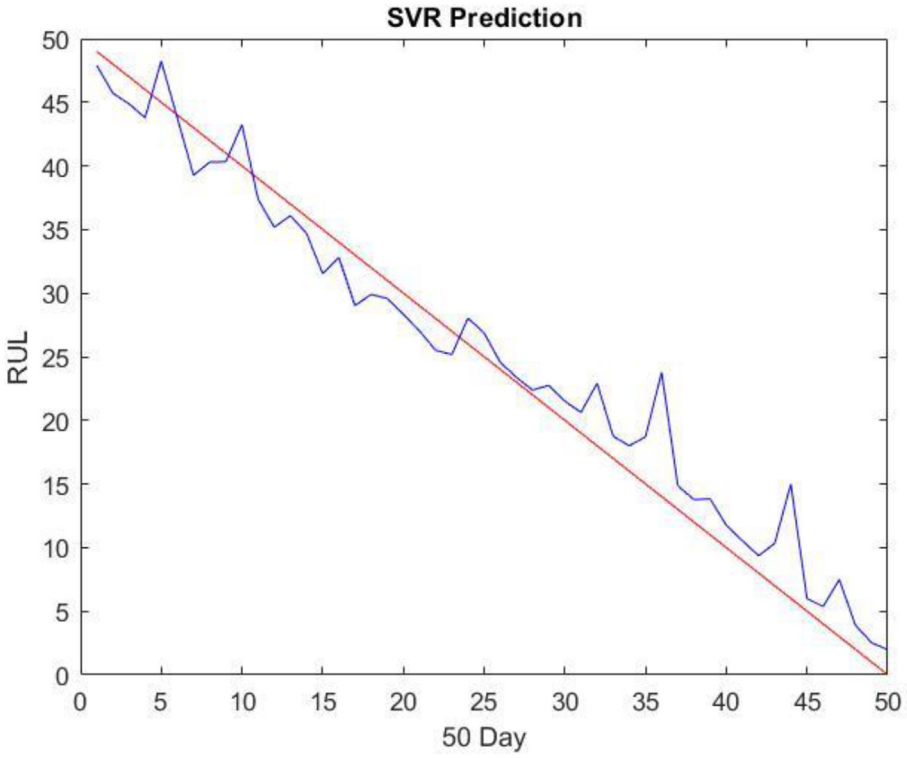

Fig. 6. SVR RUL prediction.

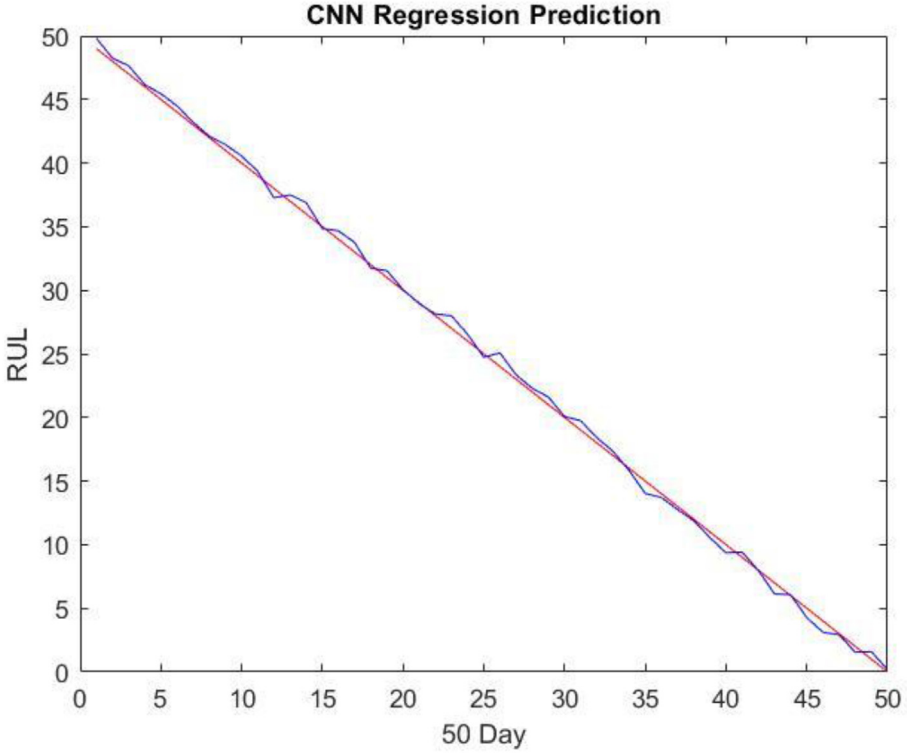

Fig. 7. CNN RUL prediction.

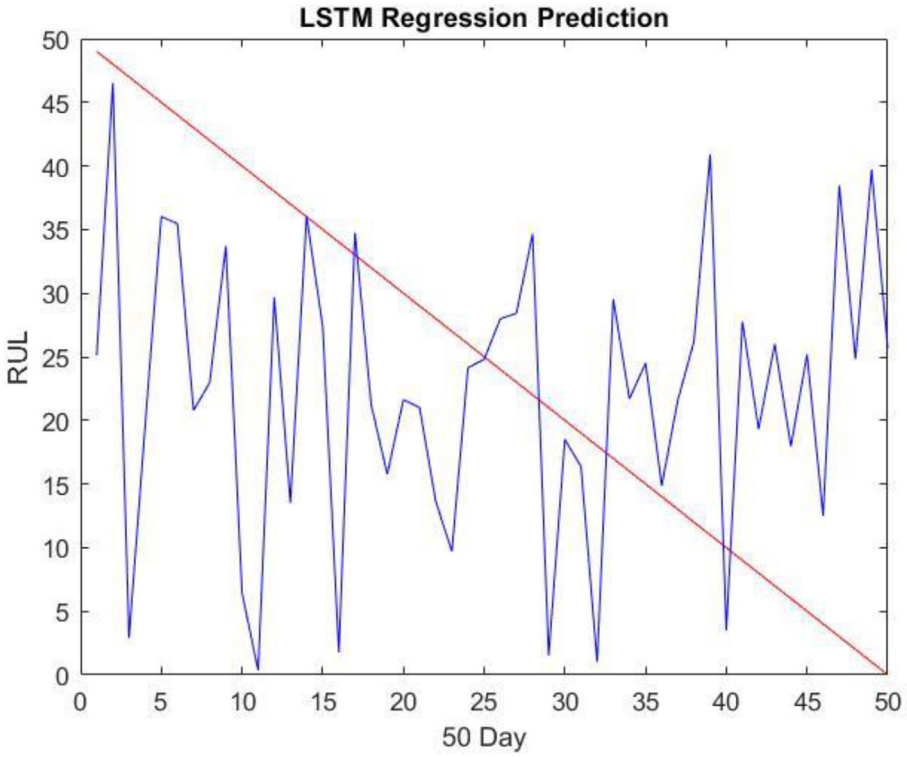

Fig. 8. LSTM RUL prediction.

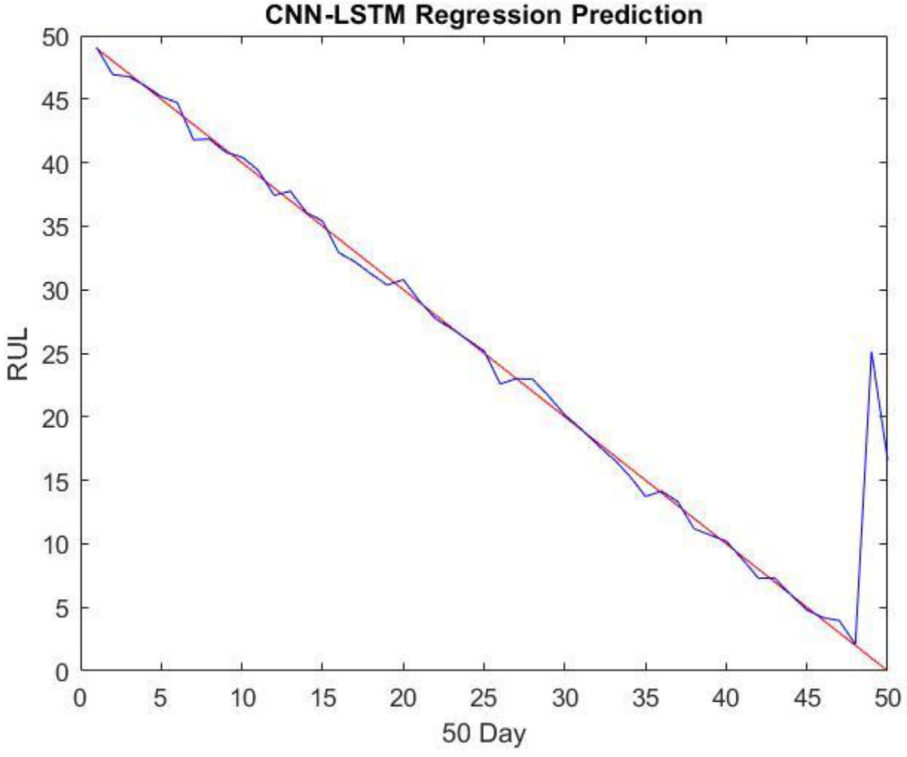

Fig. 9. CNN-LSTM RUL prediction.

Table 2. MAE comparison of predicted models.

	SVR Kernel linear	SVR Kernel polynomial	SVR Kernel Gaussian	CNN	LSTM	CNN-LSTM
MAE	4.14	2.70	2.31	0.44	14.93	1.24

Although the predictive ability of SVR is inferior to that of the CNN and CNN-LSTM models, its training speed is faster than those of all neural network-based approaches as it has the simplest model structure. In contrast, LSTM had the lowest training speed and demonstrated the worst performance.

4. Conclusion

In this study, the HSSB vibration signal of a wind turbine was used to predict the RUL, and MAE was adopted to evaluate prediction performance. Four artificial intelligence models were trained for this purpose: SVR, CNN, LSTM, and CNN-LSTM−LSTM. The simulation results of the RUL prediction by the models are summarized below.

The vibration data can be converted into the frequency domain for better feature extraction. Both frequency response plots using CNN and one-dimensional frequency domain data employing CNN-LSTM were shown to obtain a reasonably lower MAE of RUL (0.44 days for CNN, 1.24 days for CNN-LSTM), confirming that they are effective in RUL prediction. However, the construction and training of neural networks are time-consuming and complicated. In the experiment, although SVR demonstrated a slightly larger prediction MAE of 2.31 days, it was the fastest to build while obtaining reasonable RUL predictions.

Conflicts of interest

The authors declare no conflict of interest.

Acknowledgment

This work was financially supported by the ‘‘Research Center of Energy Conservation for New Generation of Residential, Commercial, and Industrial Sectors’’ from the Featured Areas Research Center Program within the framework of the Higher Education Sprout Project by the Ministry of Education (MOE) in Taiwan.

References

[1] Guo J, Zhao Y, Chen W, Zhou G. Simulation of a ship and tension Leg Platform Wind Turbine Collision. J Mar Sci Technol 2022;29(6). https://doi.org/10.51400/2709-6998.2553. Article 2.

[2] Amirat Y, Benbouzid MEH, Al-Ahmar E, Bensaker B, Turri S. A Brief Status on Condition Monitoring and Fault Diagnosis in Wind Energy Conversion Systems. Renew Sustain Energy Rev 2009;13(9):2629−36. https://doi.org/10.1016/j.rser.2009.06.031.

[3] William LC, Xing Y, Marks C, Guo Y, Moan T. Three-Dimensional Bearing Load Share Behaviour in the Planetary Stage of a Wind Turbine Gearbox. IET Renew Power Gener 2013;7(4):359−69. https://doi.org/10.1049/iet-rpg.2012.0274.

[4] Chen B, Matthews PC, Tavner PJ. Automated On-Line Fault Prognosis for Wind Turbine Pitch Systems Using Supervisory Control and Data Acquisition. IET Renew Power Gener 2015;9(5):503−13. https://doi.org/10.1049/iet-rpg.2014.0181.

[5] Yang W, Tavner PJ, Wilkinson MR. Condition Monitoring and Fault Diagnosis of a Wind Turbine Synchronous Generator Drive Train. IET Renew Power Gener 2009;3(1):1−11. https://doi.org/10.1049/iet-rpg:20080006.

[6] Saidi L, Fnaiech F. Bearing Defects Decision Making Using Higher Order Spectra Features and Support Vector Machines. In: 2013 14th International Conference on Sciences and Techniques of Automatic Control & Computer Engineering - STA; Sousse, Tunisia: 2013. p. 419−24. https://doi.org/10.1109/STA.2013.6783165.

[7] Ben Ali J, Fnaiech N, Saidi L, Chebel-Morello B, Fnaiech F. Application of Empirical Mode Decomposition and Artificial Neural Network for Automatic Bearing Fault Diagnosis Based on Vibration Signals. Appl Acoust 2015;89:16−27. https://doi.org/10.1016/j.apacoust.2014.08.016.

[8] Saidi L, Ben Ali JB, Bechhoefer E, Benbouzid M. Wind Turbine High-Speed Shaft Bearings Health Prognosis through a Spectral Kurtosis-Derived Indices and SVR. Appl Acoust 2017;120:1−8. https://doi.org/10.1016/j.apacoust.2017.01.005.

[9] Yao D, Li B, Liu H, Yang J, Jia L. Remaining Useful Life Prediction of Roller Bearings Based on Improved 1D-CNN and Simple Recurrent Unit. Measurement 2021;175. https://doi.org/10.1016/j.measurement.2021.109166.

[10] Cheng Y, Hu K, Wu J, Zhu H, Shao X. A Convolutional Neural Network Based Degradation Indicator Construction and Health Prognosis Using Bidirectional Long Short-Term Memory Network for Rolling Bearings. Adv Eng Inf 2021;48. https://doi.org/10.1016/j.aei.2021.101247.

[11] Wang B, Lei Y, Li N, Yan T. Deep Separable Convolutional Network for Remaining Useful Life Prediction of Machinery. Mech Syst Signal Process 2019;134. https://doi.org/10.1016/j.ymssp.2019.106330.

[12] Wen L, Li X, Gao L, Zhang Y. A New Convolutional Neural Network-Based Data-Driven Fault Diagnosis Method. IEEE Trans Ind Electron 2018;65(7):5990−8. https://doi.org/10.1109/TIE.2017.2774777.

[13] Merainani B, Laddada S, Bechhoefer E, Chikh MAA, Benazzouz D. An Integrated Methodology for Estimating the Remaining Useful Life of High-Speed Wind Turbine Shaft Bearings with Limited Samples. Renew Energy 2022;182:1141−51. https://doi.org/10.1016/j.renene.2021.10.062.

[14] Shaw J, Wu B. Prediction of Remaining Useful Life of Wind Turbine Shaft Bearings Using Machine Learning. J Mar Sci Technol 2021;29(5):4. https://doi.org/10.51400/2709-6998.2465.

[15] Yu PS, Chen ST, Chang IF. Support Vector Regression for Real-Time Flood Stage Forecasting. J Hydrol 2006;328(3−4):704−16. https://doi.org/10.1016/j.jhydrol.2006.01.021.

[16] Lecun Y, Bottou L, Bengio Y, Haffner P. Gradient-Based Learning Applied to Document Recognition. Proc IEEE 1998;86(11):2278−324. https://doi.org/10.1109/5.726791.

[17] Hochreiter S, Schmidhuber J. Long Short-Term Memory. Neural Comput 1997;9(8):1735−80. https://doi.org/10.1162/neco.1997.9.8.1735.

[18] Bechhoefer E, Hecke BV, He D. Processing for Improved Spectral Analysis. Ann Conf Prog Health Manag Soc 2013; 4(6).
[19] Antoni J, Randall RB. The Spectral Kurtosis: Application to the Vibratory Surveillance and Diagnostics of Rotating Machines. Mech Syst Signal Process 2006;20(2):308−31. https://doi.org/10.1016/j.ymssp.2004.09.002.
[20] Mellit A, Pavan AM, Lughi V. Deep Learning Neural Networks for Short-Term Photovoltaic Power Forecasting. Renew Energy 2021;172:276−88. https://doi.org/10.1016/j.renene.2021.02.166.
[21] Lin LH. Fault diagnosis and remaining useful life prediction of the high-speed shaft gear and bearing in wind turbine drivetrain. Taiwan: Master Thesis, Department of Mechanical and Mechatronic Engineering, National Taiwan Ocean University; 2019 (in Chinese).
[22] İnik Ö, Ceyhan A, Balcõoğlu E, Ülker E. A New Method for Automatic Counting of Ovarian Follicles on Whole Slide Histological Images Based on Convolutional Neural Network. Comput Biol Med 2019;112:103350. https://doi.org/10.1016/j.compbiomed.2019.103350.